Physics – Uspekhi **68** (7) 653 – 667 (2025)

REVIEWS OF TOPICAL PROBLEMS

PACS numbers: 61.05.F –, 61.66.Dk, **75.10. – b**, 75.30.Mb, 75.40.Gb

Neutron magnetic form factor in studies of f-electron instability

P.A. Alekseev, V.N. Lazukov, P.S. Savchenkov

DOI: https://doi.org/10.3367/UFNe.2024.09.039748

Contents

Abstract. The main results obtained in measurements of neutron magnetic form factors for rare earth systems with strong electronic correlations are presented. It is shown that in some cases neutron spectroscopy methods can provide information on the valence unstable state in the f-electron system, which is unique as regards the development of adequate physical concepts. Studies of the magnetic form factor in intermediate-valence systems based on Sm (SmB_6, SmS) and Eu ($EuCu_2Si_2$ type) and their impact on the shaping of a realistic description of the physical nature of the intermediate valence state are discussed in detail.

Keywords: neutron spectroscopy, intermediate valence, magnetic form factor, strongly correlated electron systems

1. Introduction

Over past decades, the study of the physics of strongly correlated electron systems (SCESs) based on rare-earth (RE) elements has been one of the central areas in both the experimental and theoretical exploration of condensed matter physics [1, 2]. SCESs are usually understood as systems in which the potential energy of interaction between electrons is comparable to, and in some cases significantly exceeds, their kinetic energy. A direct consequence of this circumstance is the existence of localized magnetic moments in metals and intermetallics containing ions with unfilled atomic orbitals (d or f). These substances are usually in a state with a long-range magnetic order (LRMO) at relatively high temperatures.

One of the fundamental and not fully resolved problems in the physics of f-electron, i.e., rare-earth, compounds is the phenomenon of the intermediate valence (IV) state [3–5], which in the first approximation is interpreted as a mixture of two f-electron configurations. It is believed that, in this case, a state with a non-integer population of the f-shell is realized due to the closeness in energy of two f-electron states, whose number of electrons in this inner shell differ by one. The actual situation is far from trivial: for example, for actinide (5f-electron) systems, it was proven [6] that a set of three configurations at once is possible. The key issue here is the microscopic nature of the ground state of the rare-earth ion in this case, i.e., the properties and structure of the wave function of the f-electron shell of the IV-ion.

Due to the localization in space and energy of 4f-electrons of rare-earth elements, they are a striking example of the localization (as opposed to the band) approach to the analysis of the behavior of electrons in solids [7]. Even in the metallic state, the distribution of 4f-electrons remains strongly localized in space; the Coulomb correlation is very large, and they cannot be considered by applying the band approach. For ionic compounds, a good description is provided if the 4f elements are considered in the trivalent configuration, but with some degree of covalence. Thus, as was originally shown in the early study of Freeman and Watson [8], the use of Hartree–Fock (HF) wave functions for free ions yields a good first approximation for the analysis of experiments involving 4f electron states.

These considerations underlie the use of neutron scattering to study the magnetic properties of materials containing elements with incomplete inner f- and d-electron shells. Since the neutron has a spin, and hence a magnetic moment, when scattered in matter, one of the interaction channels is so-called magnetic scattering [9], i.e., the interaction of the dipole magnetic moments of the incomplete electron shell (f- or d-type) and the neutron. This interaction can be either elastic, which implies no energy exchange between the neutron and the rare-earth ion in the solid, or inelastic, when the neutron not only changes its momentum vector, but also loses or gains

P.A. Alekseev [(1, 2, a)], **V.N. Lazukov** [(1, b)], **P.S. Savchenkov** [(1, 2, c)]
[(1)] National Research Center Kurchatov Institute,
pl. Akademika Kurchatova 1, 123182 Moscow, Russian Federation
[(2)] National Research Nuclear University MEPhI,
Kashirskoe shosse 31, 115409 Moscow, Russian Federation
E-mail: [(a)] pavel_alekseev-r@mail.ru,
[(b)] vladimir_lazukov@mail.ru,
[(c)] savch92@gmail.com

Received 2 July 2024, revised 4 September 2024
Uspekhi Fizicheskikh Nauk **195** (7) 695 – 711 (2025)
Translated by M.Zh. Shmatikov

energy due to the internal degrees of freedom of the f-electron shell. The corresponding concepts linking actually observed quantities, such as the double-differential neutron scattering cross section, with the spectral characteristics of the solid object under study, are presented in monographs and reviews, for example [9–12].

Neutron diffraction and spectroscopy are actively used to study IV systems [13] due to the wide range of options for studying the static and dynamic properties of the magnetic moment associated with f-electrons. All formulas describing the experimental results of magnetism studies using neutron scattering [14] inevitably contain the so-called magnetic form factor (MFF), which determines the dependence of the intensity of neutron magnetic scattering on the momentum transfer (Q). Since the wavelength of thermal neutrons is commensurate with the electron shell radius, interference effects arise, which determine the nature of such a dependence [4, 14]. In fact, the MFF is determined by the generalized Fourier transform of the density of the magnetic moment distribution on an atomic scale of about 0.1 nm. The main formulas linking the observed form factor with the characteristics of the state of f-electrons are presented in Section 2.1.

The generally accepted idea of valence unstable state is associated with the mixing of f-electron configurations that differ in the number of f-electrons. It is also believed that this is accompanied by partial delocalization of these electrons. Both circumstances can significantly alter the nature of the Q-dependence of the MFF, so its experimental determination is of particular importance for f-electron systems with IV [4].

Many studies exploring systems with strong electron correlations note that the IV state is formed as the hybridization of f-electrons with conduction electrons increases [13, 15, 16]. A certain pattern associated with this effect is experimentally observed, based on numerous experimental data and generally accepted model approaches. In the case of weak or insignificant (compared to the effects of the crystal electric field (CEF) and indirect exchange interaction) hybridization, the ground state of the system is determined by the relationship between these two interactions. As hybridization enhances, which is usually achieved by changing the external conditions (temperature, pressure) or the composition of the system, a number of ground state types are successively realized. They are: (a) the heavy-fermion (HF) or Kondo regime, when the CEF effects still play a certain role; (b) the Kondo insulator regime, when, as the temperature decreases, the Kondo metal turns into a narrow-gap insulator; and (c) the regime in which hybridization dominates with respect to the first two interactions. In the last case, the IV state arises, characterized by fast spin fluctuations with an energy significantly exceeding the thermal energy, $\sim k_{\mathrm{B}}T$.

Numerous neutron studies of systems of the first two (a and b) types have shown an almost complete absence of any influence of the CEF or HF state on the MFF type. Most likely, this is due to the population of the f shell remaining integer, as in case (a), or, as in case (b), changing insignificantly (virtually within the experimental error). As for changes in the angular part of the ground state wave function, due, for example, to CEF effects, the MFF is only weakly sensitive to them.

Type (c) IV-systems are characterized by a noticeable deviation of the f-shell population from the integer value, and, in some cases, this deviation is quite significant even under normal conditions (for example, SmB_6). Below, the influence of this circumstance on the MFF is discussed in detail using specific examples. Here, we only note that, as experiments (Section 2.3) and their interpretation in realistic models (Sections 2.4 and 2.5) show, the nature of the influence of IV on the features of the MFF is determined by both the physical nature of the form factor itself and the type of neutron experiment being conducted (diffraction or inelastic scattering).

It should be noted that diffraction methods for measuring the Q-dependence of the MFF are quite adequate for case (a), when a well-defined magnetic moment operates; however, in the limiting case of the IV regime (c), the situation is apparently more complicated, and it seems important to use neutron spectroscopy. This approach provides significantly more options for detailing the relationship between the contributions to the form factor and the features of the f-electron states. This conclusion, which is one of the main results of this study, provides a basis for a deeper understanding of the physical nature of the intermediate-valence state.

2. Magnetic form factor in neutron scattering

2.1 Physical nature of magnetic form factor

The sensitivity of the MFF to the character of the f-electron states is due to two main fundamental reasons related to its physical nature. First, it is the spatial distribution of the spin (**S**) and orbital (**L**) components of the magnetic moment, the combination of which underlies the formation of the total (**J**) ($\hat{\mathbf{J}} = \hat{\mathbf{L}} + \hat{\mathbf{S}}$) magnetic moment of the f-electrons of a rare-earth atom, since the spin-orbit interaction of the f-electrons for it is usually stronger than the splitting in the CEF [17]. Second, it is the physical nature of the dynamic magnetic susceptibility of the local magnetic moment $\chi(\omega, T)$. Both these circumstances determine the Fourier transform of the generalized magnetization $M(Q)$, which is present as the square of the magnetic form factor $f(Q) = M(Q)/M(0)$ in the basic formula for the intensity of magnetic scattering of neutrons on a localized magnetic moment. Its energy and momentum dependences, directly measured in the experiment, are completely determined by the so-called scattering law $S(\mathbf{Q}, E, T)$, where $\mathbf{Q}$ is the transferred momentum, $E = \hbar\omega$ is the energy transfer during neutron scattering (see below), and T is the temperature of the system.

In general, the dynamic magnetic susceptibility $\chi(\omega, T)$ is formed (1) by contributions from the Curie and Van Vleck components, respectively:

$$\chi(\omega, T) = \frac{\delta(\omega)}{k_{\mathrm{B}}T}\sum_i |D_{ii}|^2 n_i + \sum_{i\neq j} |D_{ij}|^2 \frac{(\hbar\omega_i - \hbar\omega_j)(n_i - n_j)}{(\hbar\omega_i - \hbar\omega_j)^2 - \hbar\omega^2}\,, \qquad (1)$$

where n_i is the population of the ith state with energy $\hbar\omega_i$, and D_{ij} are the dipole magnetic matrix elements linking the corresponding states.

This formula clearly shows that the physical origin of the measured magnetic dynamic or static response inevitably determines the origin and structure of the form factor. Thus, to analyze the results of neutron experiments, it is of importance to have a detailed understanding of which components of the magnetic form factor are manifested in a particular experiment.

Most often, a diffraction experiment with polarized neutrons is used to measure the MFF of paramagnets, carried out in a strong magnetic field on a single crystal [4, 18]. In this case, the induced magnetic moment of thermally populated states is measured as the difference between the intensity of the Bragg peaks for two opposite polarizations. Usually, since the measurements are carried out at sufficiently low temperatures, this is the induced moment for the ground state formed, for example, in the CEF (true for cases (a) or (b)). A more sophisticated approach to determining the MFF is associated with the analysis of the Q dependence of the intensity of certain excitations in the spectrum of inelastic magnetic scattering of neutrons, corresponding, by definition [14, 18], to the imaginary part of the dynamic magnetic susceptibility (1). The excitation spectrum, in general, contains both quasielastic and inelastic components. The signal observed in a neutron experiment, in which the MFF is also present, turns out to be associated with the susceptibility of the Curie and Van Vleck types, in accordance with the spectrum of states of the wave function of f-electrons.

For the state of an ion with a magnetic moment μ of the multiplet J, the MFF can be represented in the dipole approximation (in accordance with the notation of [4, 14]) as

$$\mu f(Q) = (\mu_L + \mu_S)\langle j_0(Q)\rangle + \mu_L\langle j_2(Q)\rangle\,.$$

Here, $\mu = g_J\mu_B J$ is the total magnetic moment, $\mu_L = (2 - g_J)J$ and $\mu_S = 2(g_J - 1)J$ are its orbital and spin components (including temperature averaging), and $\langle j_n(Q)\rangle$ are the integrals of the product of the spherical Bessel function of order n and the radial distribution of the electron density obtained from relativistic calculations in the Dirac–Fock approximation. The values of these integrals were calculated and tabulated using the HF wave functions for f-electrons in [19] for all rare-earth ions. The MFF is usually represented as

$$f(Q) = \langle j_0(Q)\rangle + C_2\langle j_2(Q)\rangle\,, \qquad (2)$$

where

$$C_2 = \frac{\mu_L}{\mu} = \frac{2 - g_J}{g_J}\,. \qquad (3)$$

It follows from the form of the expression for $\mu f(Q)$ that the contribution of $\langle j_0(Q)\rangle$ to the MFF is determined by both the spin and orbital moments, while the contribution of $\langle j_2(Q)\rangle$ only comes from the orbital moment. As an example, Fig. 1 shows the plots of the form factor components for the Nd^{3+} ion, corresponding to calculations based on the data in [19]. It is seen that the contribution from the orbital angular momentum $\langle j_2(Q)\rangle$ has a maximum at $Q \sim 6$ Å^{-1}.

The static (induced by an external magnetic field) MFF measured in a diffraction experiment is determined by the energy-integrated contributions from the magnetic susceptibility components: Curie (elastic and quasielastic excitations) and Van Vleck (intermultiplet transitions with $\Delta J \pm 1$ and intramultiplet transitions $\Delta J = 0$ ($\Delta J_z = 0, \pm 1$) between CEF levels). These components can be a source of a fairly strong dependence of the MFF on external parameters, in particular on temperature, as was shown in [18, 20, 21].

The considered representation of the MFF in the dipole approximation makes it possible to obtain quite

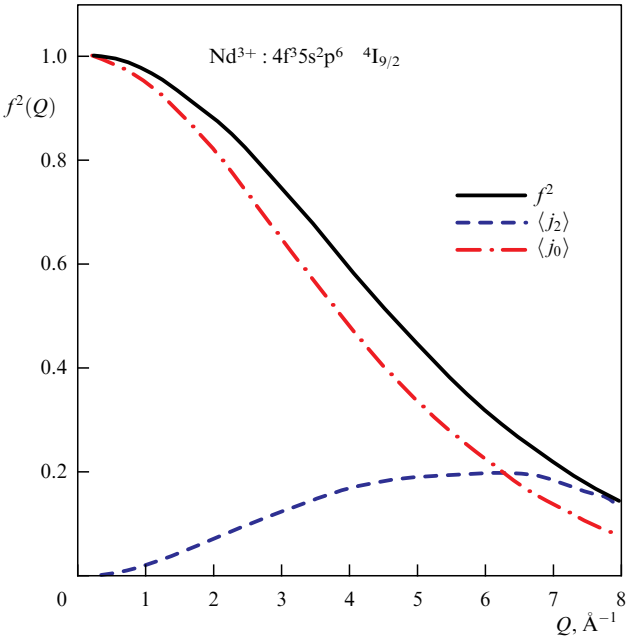

Figure 1. MFF components $f^2(Q)$ as functions of momentum transfer Q for Nd^{3+} ion. In diffraction experiment, $Q = 4\pi\sin\theta/\lambda$, where θ is neutron scattering angle, λ is neutron wavelength. (Calculation based on data in [19].)

reliable results for lanthanide compounds [22]. As shown in [20], significant deviations from the dipole approximation are only possible for large momentum transfers exceeding $Q \sim 12$ Å^{-1}. The applicability of the dipole approximation is confirmed by a large array of polarized neutron diffraction measurements on samples in an external magnetic field. Most trivalent RE ions exhibit similar static MFFs $f(Q)$ that monotonically decrease with increasing Q (the intensity drops severalfold at $Q > 6$ Å^{-1}). This is explained by a relatively small spread of positive C_2 values for intramultiplet excitations. The C_2 values range from 0 (for the purely spin J multiplet of Gd^{3+}) to 2. The only notable exception is the nonmonotonic MFF behavior for Sm^{3+} (Fig. 2) [4, 18, 23], for which the C_2 value is as large as 5.42 [20] ($C_2 = 6$ in the dipole approximation). Physically, this is a consequence of the mutual compensation of the orbital ($\mu_L = 12/7J$) and spin ($\mu_S = 10/7J$) magnetic moments for the main multiplet with $J = 5/2$. The result is the nonmonotonic behavior of $f(Q)$ noted above, which exhibits a local maximum near $Q \sim 5$ Å^{-1}.

We now consider the representation for the function describing the inelastic magnetic scattering of neutrons in a general form [24], via the dynamic magnetic susceptibility. It features a certain selectivity and allows (in contrast to the diffraction experiment mentioned above) the two main contributions to be separated. The first contribution, a Curie type, is associated with the elastic and quasielastic channels of interaction with the neutron, while the second contribution, a Van Vleck type, corresponds to transitions between the CEF levels (*intra*multiplet, $\Delta J = 0$) and/or spin-orbit levels (*inter*multiplet, limited by $\Delta J = \pm 1$ in the dipole approximation). The scattering law in this case usually looks like

$$S(\mathbf{Q}, \hbar\omega, T) = \frac{1}{2\pi}\left(\frac{g_N r_e}{\mu_B}\right)^2 \frac{\chi''(\mathbf{Q}, \hbar\omega, T)}{1 - \exp(-\beta\hbar\omega)}\,, \qquad (4)$$

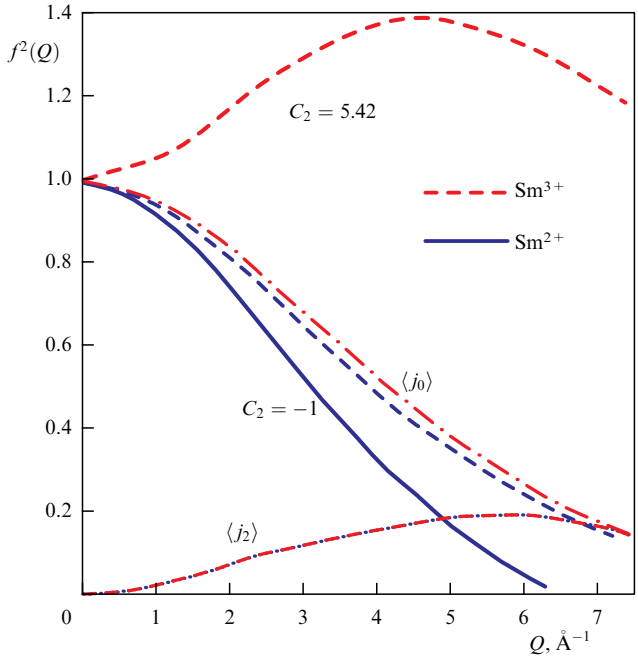

Figure 2. Calculated form factors for Sm^{2+} (solid line) and Sm^{3+} (dashed line) with $C_2 = -1$ and $C_2 = 5.42$, respectively, depending on wave vector $Q = 4\pi \sin\theta/\lambda$. Thin dashed lines represent dependences $\langle j_0(Q) \rangle$ and $\langle j_2(Q) \rangle$ (see Eqn (2)). (Taken from [23].)

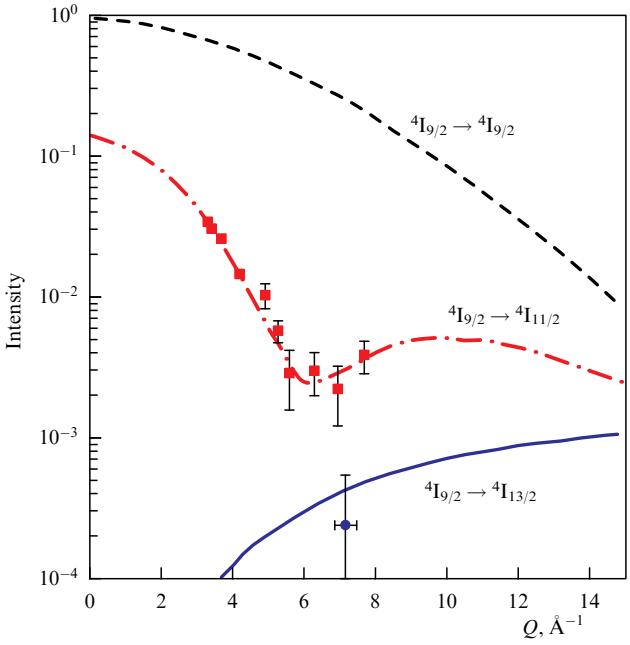

Figure 3. Neutron form factor for intermultiplet transitions in Nd^{3+}. Squares are measurements of excitation to 237 meV with initial neutron energies of 515 and 828 meV. Dot is result for excitation to 479 meV. Lines are results of calculations for corresponding excitations. (Taken from [12].)

where $\beta = (k_B T)^{-1}$, $\chi''(\mathbf{Q}, \hbar\omega, T)$ is the imaginary part of the generalized dynamic susceptibility presented above, and $g_N = -1.91$ is the gyromagnetic ratio for the neutron. Using the Kramers–Kronig relation, this value, similarly to Eqn (1), can be represented [24] as

$$\chi''(\mathbf{Q}, \hbar\omega, T) = \pi\hbar\omega \left[\sum_m f_m^2(\mathbf{Q}, T) P_{mm}(\mathbf{Q}, \hbar\omega, T) \chi_C^m(T) + \frac{1}{2} \sum_{m \neq n} f_{mn}^2(\mathbf{Q}, T) P_{nm}(\mathbf{Q}, \hbar\omega - \Delta_{nm}, T) \chi_{VV}^{mn}(T) \right], \quad (5)$$

where $P_{mm}(\mathbf{Q}, \hbar\omega, T)$ are spectral functions (Lorentzian, Gaussian, δ-function, etc.), the integral over energy of which is 1, and $f_{mn}(\mathbf{Q}, T)$ are magnetic form factors, which generally take into account correlation effects. $\chi_C^m(T)$ and $\chi_{VV}^{mn}(T)$ represent the Curie (within the state m) and Van Vleck (between the m and n states) terms in the bulk magnetic susceptibility, defined respectively as

$$\chi_C^m(T) = \frac{g_J \mu_B^2}{k_B T} \left| \langle m | \hat{J}_z | m \rangle \right|^2 \frac{\exp(-\beta E_m)}{Z}, \quad (6)$$

$$\chi_{VV}^{mn}(T) = 2 g_J \mu_B^2 \frac{\left| \langle n | \hat{J}_z | m \rangle \right|^2}{\Delta_{nm}} \frac{\exp(-\beta E_m)}{Z}, \quad (7)$$

where Z is the statistical sum.

Functional dependences of the MFF $f(Q)$ vary depending on the specific experimental conditions. Most RE intermetallic compounds demonstrate a significant influence of CEF effects on physical properties as a consequence of splitting the main J-multiplet into a certain number of sublevels, due to the symmetry of the CEF potential. Typically, the energy scale of the total splitting in the CEF for metallic systems ranges from 10^2 to 10^3 K. The splitting in the CEF, due to the differences among the energies of states with different angular distributions of electron density, has little effect on the Q-dependence of the MFF due to its physical nature.

We now outline the data on neutron studies of the form factor for intermultiplet transitions of RE intermetallics [12]. The form factor specific to this type of excitation ($\Delta J = 1$) is examined in [12, 22]. In contrast to transitions between CEF levels, spin-orbit excitations, which are associated with a mutual reorientation of the spin (S) and orbital (L) moments, correspond to an MFF of the form $\langle j_0(Q) \rangle - \langle j_2(Q) \rangle$, i.e., the value $C_2 = -1$ (see Fig. 2) in Eqn (2), and for them the dependence on Q is steeper than for the MFF of the J-multiplet.

Interest in such studies is related to the fact that the coefficient C_2 in Eqn (2) for the form factor of transitions with $\Delta J = \pm 1$, theoretically calculated in the dipole approximation, is equal to -1, as noted above. This implies that, for sufficiently large Q, exceeding 6–7 Å^{-1}, the form factor $f(Q)$ becomes negative; therefore, its experimentally measured value $f^2(Q)$ drops to zero as Q increases in the region above 6–7 Å^{-1}, and then should increase, reaching a certain maximum, and then decrease monotonically.

This theoretical result could not be verified for a long time due to the limited maximum neutron energy measurable using spectrometers at stationary reactors. The situation changed in the late 1980s, when sufficiently high-aperture neutron sources based on pulsed proton synchrotrons with a short flash, such as UK-based ISIS (RAL), became available. At this source, using a high-aperture time-of-flight spectrometer with a sufficiently high resolution ($\sim$ 1–2%), energy transfers over 200 meV and Q from 2 Å^{-1} are realized. This advancement made it possible to measure intermultiplet excitations for some rare-earth systems and obtain results consistent with theoretical calculations. Figure 3 presents, as an example, experimental data for the Q dependence of the intensity (determined by the form factor $f^2(Q)$) of intermultiplet

transitions of the Nd^{3+} ion, in particular, the $^4I_{9/2} \rightarrow {}^4I_{11/2}$ transition with an energy of 237 meV.

It should be noted that precisely the 'light' RE elements are the most convenient ones for such measurements: the energy of the first J-multiplet is not too high (250–290 meV), which allows obtaining fairly small Q. On the other hand, it is beyond the phonon spectra, which increases the accuracy of measuring the intensity of the magnetic signal. Energies of intermultiplet transitions of 'heavy' REs are significantly higher, and this circumstance complicates the experiment. RE elements in the middle of the series are 'plagued' not only by problems due to strong neutron absorption, which requires using isotopically pure materials, but also by problems related to taking into account the phonon contribution.

The IV state is characteristic primarily of the elements of the beginning (Ce), middle (Sm, Eu), and end (Tm, Yb) of the rare-earth series, which is usually associated with the relative instability of such electron configurations (of type $f^0 \leftrightarrow f^1$ or $f^5 \leftrightarrow f^6 \leftrightarrow f^7$, or $f^{13} \leftrightarrow f^{14}$, respectively). The specific feature of the IV state is most clearly manifested in the results of spectroscopic experiments with different time resolutions. For example, a 'fast' X-ray spectral experiment (L_3 edge, XANES, characteristic time $\tau \sim 10^{-15} - 10^{-17}$ s) yields two peaks in the spectrum, corresponding in position to the configurations f^n and $f^{n\pm1}$, while a slow experiment (isomeric shift in the Mössbauer effect $\tau \sim 10^{-9}$ s) yields a single peak at an intermediate position. This means that the rate of interconfiguration fluctuations [5] lies in the region $\tau \sim 10^{-10} - 10^{-14}$ s. It should be noted that, in a neutron spectroscopic experiment, $\tau \sim 10^{-11} - 10^{-13}$ s, and this scale provides a unique opportunity [13, 15, 24] to directly observe and study spin fluctuations characteristic of IV ions.

Splitting under the action of CEF usually does not manifest itself against the background of configurational instability of the J-multiplet, and the corresponding excitations are not visible in a neutron spectroscopic experiment with IV systems. However, spin-orbit intermultiplet ($J \leftrightarrow J \pm 1$) transitions can be observed [25–27]; these excitations are related to the Van Vleck magnetic susceptibility (7).

According to realistic calculations of the radial electron density distribution [19], the values of $\langle j_0(Q) \rangle$ and $\langle j_2(Q) \rangle$ for adjacent 4f configurations, such as f^5 (Sm^{3+}) and f^6 (Sm^{2+}) [28], differ only slightly. Consequently, the identity of the C_2 value implies very similar Q-dependences of the MFF, which was confirmed experimentally for spin-orbit transitions measured for the IV systems SmB_6 [25, 29, 30] and Sm(Y)S [31]. A similar character of the Q dependence was observed in [32] for the excitation of $J = 0 \rightarrow J = 1$ and, in the case of an integer valence for Sm^{2+}, in the semiconductor compound SmS. We emphasize that the peaks in the spectra of inelastic magnetic neutron scattering observed in the above experiments are associated with dipole transitions from the ground state to the excited state, which correspond exclusively to the Van Vleck contribution to the dynamic susceptibility.

On the other hand, it can be expected that the quasielastic signal due to the Curie component of the dynamic magnetic susceptibility contains information on the properties of the wave function of the states populated at a particular temperature. This selectivity predetermines the differences among the form factors of various parts of the magnetic excitation spectrum. In contrast to the diffraction studies of the magnetic field-induced MFF mentioned above, this case provides information on the unperturbed (by the external magnetic field) wave function.

An essential feature of the IV state is almost always the presence of fairly fast spin fluctuations ($10^{-11} - 10^{-13}$ s), which, at first glance, naturally and inevitably rules out the possibility of implementing a long-range magnetic order for the RE sublattice in such a system. However, in some cases, their coexistence in a certain region of the phase diagram of the IV system is experimentally observed [16, 33].

The phenomenon of intermediate valence was first experimentally discovered in samarium hexaboride [34]. Later, this system and its derivatives were actively studied by various methods, including neutron spectroscopy [13, 35]. This allowed the formulation of certain physical concepts of the IV phenomenon at the microscopic level (see Section 2.4).

It should be noted that the greatest number of systems exhibiting the IV state contain cerium [3, 12], including both pure Ce ($\gamma \leftrightarrow \alpha$ transition under pressure) and a number of its compounds: $CeNi_5$, $CePd_3$, $CeSn_3$, etc. Neutron studies of IV states were also carried out for systems based on ytterbium (end of the RE series), samarium, and europium (middle of the series). The IV state was also observed and analyzed in [6] in actinide systems.

Below, specific examples of neutron studies of the MFF in various rare-earth systems are presented to analyze their connection with the specific features of the IV state.

2.2 Neutron form factor for intermediate-valence systems based on cerium and ytterbium

We now proceed to the measurements of the magnetic form factor of the IV ion of cerium carried out for intermetallics. These are mainly diffraction experiments (induced magnetic moment and polarized neutrons), which are discussed in detail in [3].

The results obtained show good agreement between the Q dependence of the experimental values of $f(Q)$ and calculations using the model presented in Section 2.1 and adopted in most studies of cerium systems as the basis for calculating the MFF for the Ce^{3+} ion. Such measurements were carried out and analyzed for $CePd_3$ (the valence estimated from L_3-edge measurements is $v = 3.15$) and $CeSn_3$ ($v \sim 3.05$); for the former system, the results of neutron diffraction measurements [36] are presented in Fig. 4.

It should be noted that the Ce^{4+} configuration has no f-electrons and, from general considerations, one could expect either a change in the nature of the Q dependence for the IV state (to be steeper relative to Ce^{3+}) due to possible 'delocalization' of the f-electron or the addition of a corresponding contribution from the competing electron shell (d-, p-, s-?), or a decrease in the absolute amplitude of the signal relative to the case of the initial Ce^{3+}. The latter option seems more realistic, but its experimental observation, like any absolute measurement of intensity, is more problematic. Similar results were obtained for $CeSn_3$ [37] and for the $\gamma \rightarrow \alpha$-transition to the IV state for Ce, realized in neutron experiments on the $Ce_{0.74}Th_{0.26}$ system [38].

The results displayed in Fig. 4, which are discussed in [36], are typical of cerium IV systems in terms of the influence (or rather, the virtual absence) of the IV state on the observed form factor associated with the ground J-multiplet. Two main circumstances characteristic of cerium systems should be noted: (1) the character of the Q dependence of MFF virtually, within the limits of experimental error, corresponds to that expected for a normal $4f^1$ shell; (2) the form

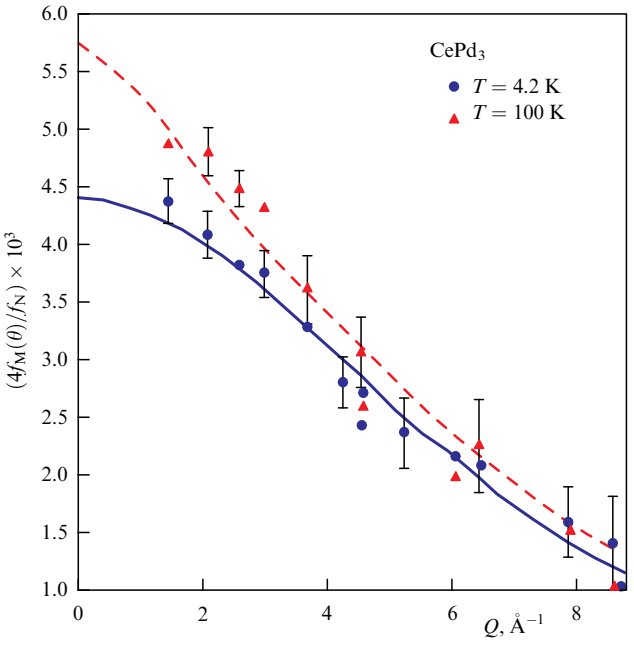

Figure 4. Magnetic form factor (f_M) squared of $CePd_3$ single crystal measured in a diffraction experiment with polarized neutrons [36] at $T = 4.2$ K and $T = 100$ K, presented as a function of wave vector Q. Solid line is fit of $f^2(Q)$ for Ce^{3+}; dashed line corresponds to inclusion of an additional contribution to MFF from 5d electrons (17%). Intensity of f_M is normalized to that of the nuclear Bragg peak f_N. (Taken from [36].)

factor amplitude decreases due to the deviation of the valence from an integer to decreasing shell population, but weaker than can be expected based on direct measurements of the valence value. The additional contribution to the MFF at a low temperature was not unambiguously correlated with the specific effect, which is apparently due to the rearrangement of the spectrum of magnetic excitations with decreasing temperature discovered later [26, 27]. These circumstances are still not fully understood to this day.

The urgency of this problem is somewhat alleviated by an even stranger, but indisputable, observation. The fact is that even in systems where the formal valence of cerium is apparently 4+ (for example, the ionic compound CeO_2, or $CeNi_5$), the spectroscopic experiment (L_3-edge) yields valence v of no more than $v = 3.4$. The issue of the relationship between the concepts of the numerical valence of cerium as applied to various methods of its determination remains open. In our case, as applied to rare-earth intermetallic compounds, the categories of 4f-shell states (a), (b), and (c), presented in the Introduction, seem to be fairly reliable guidelines for classification.

Systems based on Yb (the end of the RE series) are considered representatives of the IV-type state $f^n \leftrightarrow f^{n+1}$ ($f^{13} \leftrightarrow f^{14}$), which is physically analogous to the case of cerium systems, since it corresponds to fluctuations between magnetic and nonmagnetic configurations. Here, the systems YbCuAl, $YbAgCu_4$ [39], $YbCu_2Si_2$, $YbPd_2Si_2$ [40–42], and $YbAl_3$ have been studied the most. The form factors of Yb in these systems have not been examined, and quantitative spectroscopic measurements of its valence (L_3-edge, isomer shift) give a value that slightly (in fact, within the experimental error) differs from 3+ $(3 - \delta)$. Inelastic peaks (correlated with CEF effects) are observed in the neutron spectra [3] of these systems, along with a fairly wide (up to 40 meV) quasielastic signal, significant at temperatures above 50–100 K. Evaluating these results from modern positions, it can be assumed that Yb systems can be classified as Kondo insulators [43] by the nature of the neutron spectra, with the formation of a spin gap, but without a metal–insulator phase transition. The applicability of such an approach was, in particular, substantiated for $YbAl_3$ in a detailed neutron study [44].

We especially note the YbB_{12} system, known as an example of a 'classical' Kondo insulator [13, 43, 45–49]. The valence of Yb in this system, determined from L_3-edge X-ray spectroscopy data, as in the cases considered above, differs only slightly from 3+ to the lower side. In this system, a metal–insulator transition is observed at $T \leqslant 80$ K. Detailed neutron studies on both poly- and single-crystal samples using polarization analysis made it possible to clearly understand the nature of the magnetic excitation spectrum, its temperature evolution, and the effect of substitution in both sublattices [43, 50, 51]. It was noted that the nature of the Q dependence of all features in the magnetic neutron scattering spectrum associated with excitations of the ground $J = 7/2$ multiplet is consistent with the corresponding form factor when taking into account the influence of modulation due to cooperative effects.

2.3 Neutron form factors for intermediate-valence systems based on samarium and europium

2.3.1 Physical features of Sm and Eu IV systems. We now proceed to the results of studying IV systems based on RE elements close to the middle of the f-element series. The conditions for the formation of the intermediate-valence state in this case are qualitatively different from the previously considered situation of the beginning and end of the RE series. Here, two partially filled f-shells compete: in the case of samarium, they are f^5 and f^6 ($Sm^{3+} \leftrightarrow Sm^{2+}$), and for europium, they are the states f^6 and f^7 ($Eu^{3+} \leftrightarrow Eu^{2+}$).

Each of these f-shell configurations, differing in the number of electrons, has its own magnetic ground state due the spin-orbit interaction. The f^6 configuration corresponds to the singlet ground state $^7F_0$ ($J = 0$), separated from the higher $^7F_1$-state with $J = 1$ (spin-orbit triplet) by an energy of 36 meV in the case of Sm^{2+} and by 45 meV for Eu^{3+}, respectively. The f^5 configuration corresponds to the ground multiplet $^6H_{5/2}$, separated by an energy of 125 meV from the nearest multiplet $^6H_{7/2}$. The f^7 (Eu^{2+}) state qualitatively differs from all the previous ones, since for it the orbital moment of the shell is absent ($L = 0$), and the spin moment has the maximum value $S = 7/2$, just as for the Gd^{3+} ion. From this observation, it follows, to a first approximation, that, for the state $^8S_{7/2}$ corresponding to the f^7 configuration, there is no spin-orbit interaction, nor are there any CEF effects. Note that for both lower multiplet states f^5 and for the f^6 state with $J = 1$ (Sm^{2+} and Eu^{3+}), CEF effects can, in principle, occur.

All these factors manifest themselves to some extent during the formation of the IV state, determining, in particular, the properties of the ground state of the IV ion and the specific spectrum of its excitations. It should be noted that the relatively low spin-orbit splitting energy compared to other RE ions (including Ce, Pr, Tm, and Yb) provides additional options to use neutron spectroscopy to study the features of intermultiplet transitions in samarium and europium IV compounds.

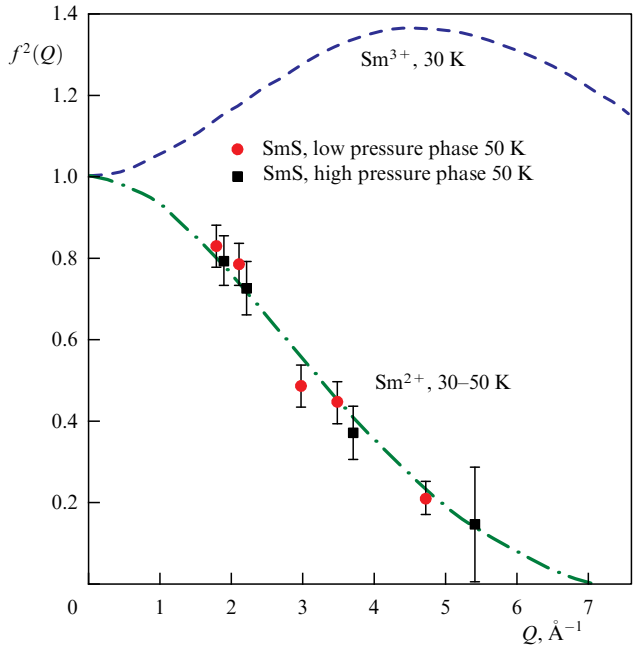

Figure 5. Induced magnetic form factor $f^2(Q)$ of Sm in SmS ($P = 0$: dots, $P = 0.6$ GPa: squares) measured in a neutron diffraction experiment with polarization analysis at $T = 30$ K. Calculation: Sm^{2+} — dashed-dotted line, Sm^{3+} — dashed line. (Taken from [28].)

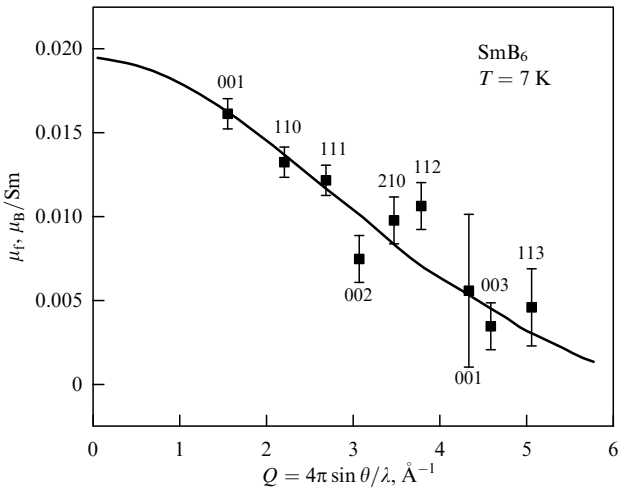

Figure 6. Induced magnetic form factor $f^2(Q)$ of Sm in SmB_6 measured in a neutron diffraction experiment with polarization analysis at $T = 7$ K and a magnetic field of 5 T (doubly isotopic sample ^{154}Sm, ^{11}B). Line represents calculation of Sm form factor with $C_2 = -1$ (From [23].)

One cannot help but note the specific problems of these elements due to the strong absorption of thermal neutrons for the natural isotopic composition of Sm and Eu. Therefore, notably, all neutron experiments with samarium samples were carried out using the ^{154}Sm isotope.

2.3.2 Static magnetic form factor of SmS. The first in the considered group of compounds to be measured by polarized neutron diffraction was the induced magnetic form factor of the samarium ion in the IV state (the so-called 'golden' phase of SmS), realized in two ways: in the pure SmS system under a pressure of 0.6 GPa and in the $Sm_{0.75}Y_{0.25}S$ system [28], where the IV state was achieved by 'chemical compression' under normal conditions. The valence of samarium is estimated to be close to $v \sim 2.5$ in both cases. The results of one of these experiments are presented in Fig. 5.

The result of the experiment turned out to be indisputable and at the same time paradoxical and unexpected due to the absence of signs of a Curie contribution from Sm^{3+}, which contradicted the then existing concepts of the IV state [15, 28]. This circumstance, along with the results of studies of the phonon spectra of these two systems [28, 52], facilitated the development of more adequate theoretical models [53, 54], which linked particularly phonon anomalies with the intermediate-valence state related to the so-called resonance violation of the adiabatic approximation — the main postulate in the theory of solid state dynamics.

2.3.3 Static magnetic form factor of SmB_6. The intermetallic compound SmB_6 is a 'pioneer' in the physics of IV-systems; it was in this compound that the intermediate-valence state was discovered (see above). This system, which is characterized by a valence of $v = 2.5$ under normal conditions, demonstrates that valence can vary upon substitution in the rare-earth sublattice [13]. The application of external pressure does not exert a strong effect on the valence state up to 10 GPa [55].

The neutron form factor for the induced magnetic moment in SmB_6 was measured in a polarized neutron diffraction experiment on a single crystal in a magnetic field of 5 T at a temperature of 7 K at the Leon-Brillouin Laboratory (Laboratoire Léon Brillouin, LLB) (spectrometer 5C2, Saclay, France) [23]. The result (Fig. 6) essentially coincided with that obtained earlier for the IV state in SmS (see Fig. 5). In fact, the experiment agrees with the dependence on Q, characteristic of the form factor of the intermultiplet transition $J = 0 \rightarrow J = 1$ for Sm^{2+}, shown by the solid line in Fig. 6. Note that absolute normalization allows estimating the value of the effective magnetic moment, which turned out to be about $0.02\mu_B$. Such a small value also indicates the Van Vleck origin of the magnetic susceptibility as the most probable source of the induced moment of this paramagnet.

In analyzing the results for the SmB_6 and SmS systems, the following circumstances should be additionally noted. The authors of [28] attempted to explain such an unexpected result for SmS by the presence of a strong temperature dependence for the MFF of Sm^{3+} due to the effects of the crystalline electric field and spin fluctuations (in a certain sense, these phenomena are mutually exclusive). The extremely low value of the induced magnetic moment in Sm, obtained experimentally in [23], almost excludes the admixture of the Sm^{3+} configuration (irrespective of any influence of the hypothetical CEF effects) with a magnetic moment of $\sim 0.8\mu_B$. The presented paradoxical results, taking into account the value of $v \sim 2.5$, allow us to assume that the nature of the IV state of the two samarium systems is to some extent the same and indicate that a common approach can be used to analyze the nature of the ground state of Sm in these systems. To implement this option, we examine the results of detailed spectroscopic studies on poly- and single-crystal samples using the time-of-flight technique and three-axis spectrometers, respectively.

2.3.4 Inelastic neutron scattering spectra in SmB_6 and Sm(Y)S. Spectra of inelastic neutron scattering on SmB_6 were initially measured to study intermultiplet transitions for two competing configurations: Sm^{2+} and Sm^{3+}. The measurements were

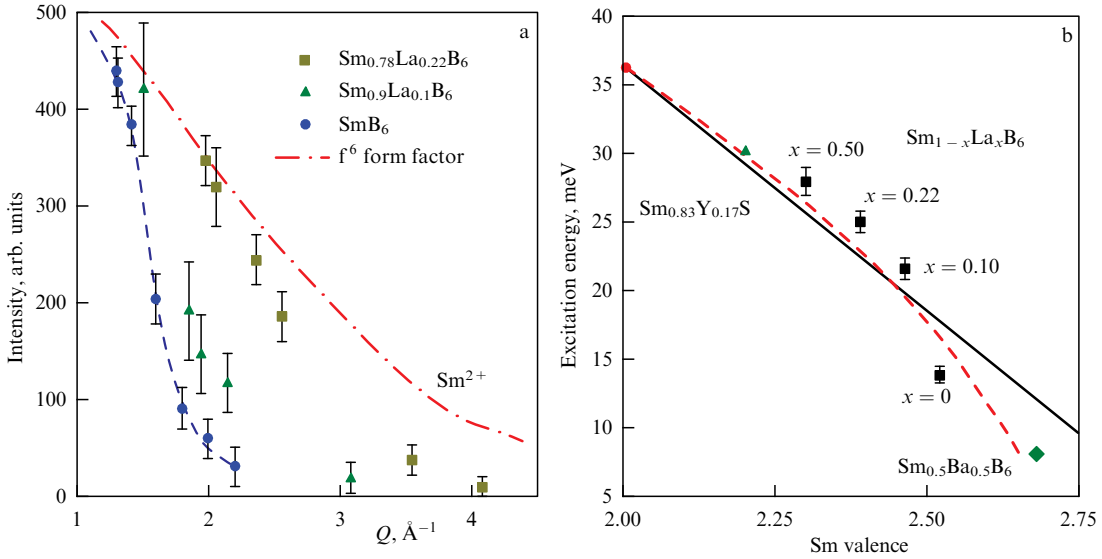

Figure 7. Parameters of resonance mode for $(Sm, M)B_6$ systems. (a) Dependence of intensity on momentum transferred along [111] direction. (b) Energy of resonance mode depending on average valence of Sm (at $T = 10$ K). Solid line is calculation made according to the model [58], dashed line is drawn for viewing convenience. (Taken from [57].)

carried out with the HET time-of-flight spectrometer of the ISIS pulsed neutron source (RAL), which provided a wide range of energy and momentum transfer at high energy resolution. It should be stressed immediately that we do not discuss the procedure for separating the magnetic and phonon components of the spectra (their energy ranges overlap); this issue is discussed in detail in the original publications [25, 29, 30, 56, 57]. Below, we only consider the magnetic components of the neutron spectra.

The peaks of inelastic magnetic scattering were detected at energies corresponding to those of intermultiplet transitions for the f^6 and f^5 configurations, respectively, for Sm^{2+} (36 meV) and Sm^{3+} (125 meV). The ratio of their intensities turned out to be directly related to the average valence. This was confirmed by the results of measurements with samples where the samarium valence was varied by substitution in the RE sublattice [57]. We emphasize that the intermultiplet transitions correspond to the Van Vleck component of the dynamic magnetic susceptibility.

The nature of the dependence of the peak intensity on the momentum transfer turned out to be in agreement with that expected for the form factors of the corresponding intermultiplet transitions [57]. The same behavior of the Q dependence was obtained in [32] for $J = 0 \to J = 1$ excitation of the stable Sm^{2+} ion in SmS. An important feature of the SmB_6 spectra is the very large energy width of these peaks (~ 20 meV at $T \sim 10$ K), which significantly exceeds the instrumental resolution and corresponds to the scale of fast spin fluctuations with a period of $\tau \leqslant 10^{-12}$ s. It can be concluded that these states do not represent the true ground state of suchlike IV systems.

In general, the spectra of spin-orbit excitations did not exhibit any unexpected effects, in contrast to the region of relatively low energy transfers. In this energy region, one would expect manifestations of quasielastic scattering due to scattering on the lower multiplet for Sm^{3+}, instead of transitions between CEF levels suppressed by spin fluctuations. The specific feature of the Q dependence of the MFF for $J = 5/2$ (see Section 2.1) provides this type of excitation with a three- to fourfold gain with respect to the MFF of spin-orbit excitation in its spectral region. Despite the significantly smaller value of the magnetic scattering cross section ($\sigma_m = 0.4$ b) for the $J = 5/2$ multiplet compared to the transition $J = 5/2 \to J = 7/2$ ($\sigma_m = 2.4$ b), this suggested a quite observable intensity of quasielastic scattering (expected width of 15–20 meV) in the region of positive energy transfers at low temperatures, near the elastic peak from nuclear scattering. Nevertheless, in the experimental spectra at low temperatures, no signs of a quasielastic signal were observed. Apparently, this circumstance is in line with the absence of traces of the MFF from Sm^{3+} in the diffraction experiment.

The observation in the neutron scattering spectrum of SmB_6 of a rather intense and very narrow (the width is of the order of the instrumental resolution) peak at an energy of about 14 meV (the so-called 'resonance' mode) was an important and rather unexpected event. Its intensity sharply decreased as the momentum transfer increased, i.e., when comparing the spectra measured at different neutron scattering angles. The negligibly small intrinsic width clearly indicates its connection with the electronic spectrum of the ground state of the system, in contrast to the short-lived mutually competing f-electron states. This was confirmed by experiments [57] carried out on polycrystalline compounds $Sm_{1-x}La_xB_6$, where the connection of the characteristics of this excitation, i.e., energy and form factor, with average valence was studied (Fig. 7).

Extrapolation of the measurement results to the valence $v = 2+$ indicates that the parameters indicated match the values characteristic of the f^6 configuration for both $f^2(Q)$ and the spin-orbit excitation energy (36 meV). It can be assumed that, in the IV state for Sm, the neutron spectrum exhibits excitation from a new ground state of the system with the total angular momentum J^*, whose nature of excitation is similar to $J = 0 \to J = 1$. This assumption was confirmed by detailed neutron studies [31] on $Sm_{1-x}Y_xS$ single crystals in the IV state. As neutron spectroscopy [32] has shown, the spin-orbit excitation for the f^6 configuration of Sm is weakly dispersive due to a certain level of the Sm–Sm exchange interaction existing in SmS. In [31], dispersion relations were studied for the excitation $J = 0 \to J = 1$ and for the low-

energy peak (conventionally designated as $J^* = 0 \to J^* = 1$), similar to the 'resonant' mode observed in SmB_6 and 'related' systems $Sm(La)B_6$. It turned out that, within the Brillouin zone, the dependences of the energy and intensity on the wave vector for these two excitations in Sm(Y)S are strongly interrelated. This clearly indicates their symmetry identity and, consequently, the singlet nature of the 'true' ground state of the system, and, hence, explains the absence of a quasielastic signal and a Curie contribution to the form factor at the low temperatures noted above.

The properties of low-energy magnetic excitation (resonant mode) were studied in detail by neutron spectroscopy methods on a unique doubly isotopic single crystal of SmB_6. It turns out that this excitation features not only a unique form factor that rapidly decreases with increasing Q, but also a strongly restricted topology of its existence in the momentum space [13, 56]. In fact, this excitation is only observed near highly symmetric regions of the momentum space, i.e., near the boundaries of the first Brillouin zone (points $\mathbf{R}(1/2, 1/2, 1/2)$ and $\mathbf{X}(1, 0, 0)$) and those closest to it ($\mathbf{X} + \mathbf{G}$, where $\mathbf{G}$ is the reciprocal lattice vector) [58]. The presence of a signal near certain points of the momentum space indicates the existence of correlation effects. As shown in [58], most likely this can be interpreted based on the 'topological insulator' concept applicable to the SmB_6 system when considering its low-temperature properties.

2.3.5 Form factor of quasielastic neutron scattering in SmB_6. We now consider the results of a study of the MFF for the quasielastic spectral component of the dynamic magnetic susceptibility of SmB_6 first obtained in [59]. This component of the neutron magnetic scattering spectrum has not previously been investigated either in SmB_6 or in SmS. On the one hand, it is the most probable carrier of the Curie component of the dynamic susceptibility, and on the other hand, it directly reflects the spin relaxation (fluctuations) due to the interaction of f-electrons with the environment, which are very specific to IV-systems.

The experiments were carried out at LLB on a doubly isotopic single crystal $^{154}Sm^{11}B_6$ (previously used in [23, 56–58]) using a 2T high-aperture three-axis crystalline spectrometer. This provided reliable separation of the magnetic quasielastic component against the background of nuclear inelastic and elastic scattering.

The quasielastic component in neutron scattering only appears at temperatures above 80 K, and its intensity is uniformly distributed over the momentum space. Apparently, for this reason, diffraction experiments turned out to be virtually insensitive to it due to the low signal-to-noise ratio.

Along with the magnetic quasielastic signal, in experiments using spectroscopy in the energy transfer region of up to 20 meV, a phonon component was observed from both the density of states and the coherent neutron scattering, which is due to the acoustic and lower optical branches, and the contribution of this signal increases sharply with increasing Q. Since the intensity of the magnetic quasielastic signal is measured to study the dependence on the transferred momentum, an additional competing contribution from phonons is extremely undesirable. It can be reliably excluded only by using a single crystal, which allows employing the measurement points of the q space that are virtually free of the phonon contribution due to the complete suppression of the incoherent scattering amplitude in ^{154}Sm and the smallness of this value in ^{11}B. This methodology enabled us to solve the problem of studying the magnetic form factor of quasielastic scattering in SmB_6.

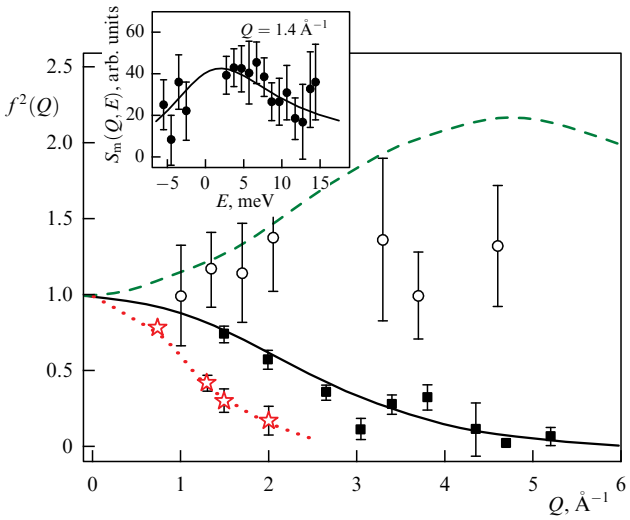

Figure 8. Experimentally determined Q dependences of various components of magnetic signal for IV system SmB_6. Stars are resonance mode (excitation at 14 meV and $T = 2$ K) [56]; squares are static form factor from diffraction study [23] ($T = 7$ K); circles are normalized intensity of the quasielastic signal measured at $T = 100$ K [59]. Dashed line represents calculation (Eqns (2) and (3)) of static MFF for main multiplet of Sm^{3+} at $T = 0$; solid line is calculation of MFF for Sm^{2+} (in fact, this is the Van Vleck contribution to diffraction form factor from spin-orbital excitation); dotted line is drawn for viewing convenience. Inset shows experimental data on magnetic quasielastic signal obtained as difference between neutron spectra measured at 100 K and 2 K, $Q = 1.4$ Å^{-1}, line is fit of spectral function by a Lorentzian with a half-width at half-maximum of $\Gamma_{QE}/2 = 8(2)$ meV. (Taken from [59].)

Figure 8 shows the measured intensity of the quasielastic signal as a function of momentum transfer, along with the measured intensity of the peak at $E = 14$ meV and the calculated MFF for the spin-orbit excitation and ground state of Sm^{3+}. The data displayed in Fig. 8 show a striking difference between the experimental Q dependences of the various components of the magnetic signal in neutron scattering, even despite the significant spread of the experimental points for the quasielastic signal due to its relatively low intensity. It is of interest to note that none of these components exhibits the specific Q dependence characteristic of the $J = 5/2$ multiplet of Sm^{3+}.

2.3.6 Neutron magnetic scattering spectra on the IV system $EuCu_2Si_2$. The intermetallic compound $EuCu_2Si_2$ is one of the first europium-based compounds where the IV state of its f-electron shell was discovered [60–62]. This compound and systems based on it and related compounds of the 1−2−2 type are of interest due to the high lability of the IV state. It features high sensitivity to changes in both composition and even temperature [61, 62]. As noted above, in this compound, the basis for the IV state consists of two f-electron configurations: f^6 and f^7. The latter corresponds to exactly half the filling of the f-shell, due to which it is relatively stable, ensuring the stability of the state of the corresponding Gd^{3+} ion. Additional interest in the study of the $EuCu_2(Si_{1-x}Ge_x)_2$ and $EuCu_2Si_2$ systems is also associated with the possible existence of a quantum critical point and the possibility of observing a quantum phase transition discussed in recent studies [63, 64]. The quantum phase transition can be induced

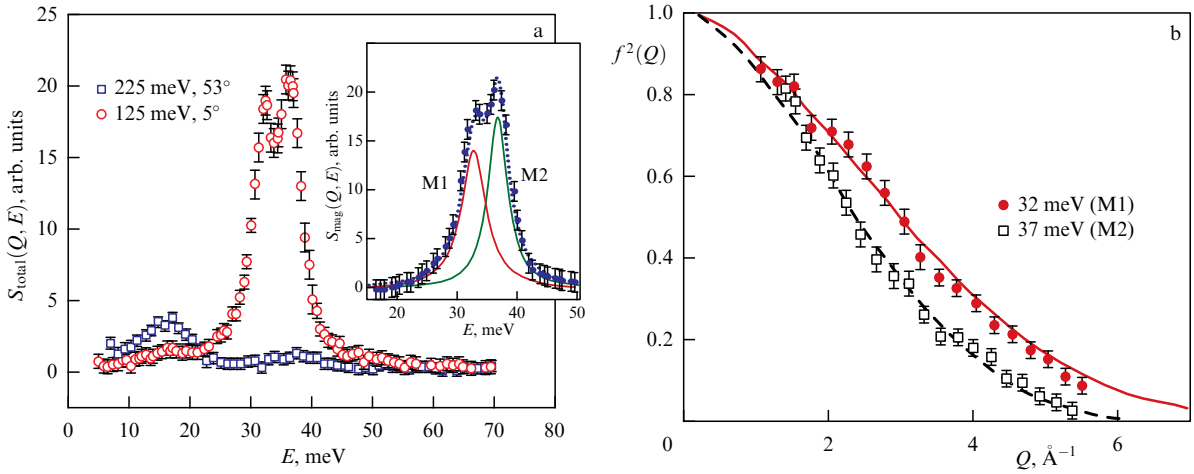

Figure 9. (a) Spectral neutron scattering functions of $EuCu_2Si_2$ measured at minimum momentum transfer ($Q_{min} = 0.6$ Å^{-1}), $E_i = 125$ meV, $2\theta = 5°$ (dots), and maximum momentum transfer ($Q_{max} = 10$ Å^{-1}), $E_i = 225$ meV, $2\theta = 53°$ (squares). Inset shows fit of magnetic component ($S_{mag} = S_{total} - S_{ph}$) of spectrum by two Lorentzians with energies of 32 and 37 meV; (b) Q-dependences of intensities of magnetic peaks at 32 meV (M1, dots) and 37 meV (M2, squares) and their comparison with form factors $f^2(Q)$ for degenerate state f^7 (solid line) and intermultiplet transition for f^6 (dashed line) (see text). (Taken from [74].)

by both chemical substitution in $EuCu_2(Si_{1-x}Ge_x)_2$ and hydrostatic pressure in $EuCu_2Ge_2$, and is also observed in some related europium systems of the 1–2–2 type [65–68].

The configuration characteristics of the IV state of europium are essentially close to those of the IV state of samarium, being in some aspects even physically simpler. First and foremost, we note that, for the ground states of both electron configurations, Eu^{2+} and Eu^{3+}, CEF effects are excluded. The spin-orbit excitation energy of singlet-triplet transition $J = 0 \to J = 1$ for Eu^{3+} is 46 meV, which is slightly higher than for Sm^{2+} (36 meV). The f^7 configuration for Eu^{2+} has no orbital momentum or corresponding dipole excitations, so its magnetic susceptibility corresponds exclusively to the Curie type.

The first neutron measurements of the magnetic excitation spectrum of a number of IV-type 1–2–2 systems based on europium [69–71] generally confirmed these ideas. Our studies of $EuCu_2(Si_{1-x}Ge_x)_2$ [72–74] with a higher experimental resolution and an extended range of momentum transfer Q due to the use of a time-of-flight spectrometer at the ISIS pulsed neutron source (RAL) allowed us to reveal important details.

First and foremost, it was found in $EuCu_2Si_2$ that, in the neutron spectrum at $T = 7$ K (the valence of europium $v = 2.84$), there is no quasielastic magnetic scattering (contrary to what is expected for the contribution from the purely spin state f^7); instead, there is a spin gap, and the quasielastic component of the spectrum only appears at temperatures $\geqslant 100$ K. It also turns out that, at an energy of 46 meV, where the spin-orbit transition for Eu^{3+} should be located, there is no magnetic peak, but there are two magnetic peaks of close intensity at energies of 37 and 32 meV. We analyzed in detail their properties in comparison with those of SmB_6 in [74].

Experiments involving the detailed study of the form factors of these excitations were conducted on the SEQUOIA spectrometer of the spallation neutron source (SNS) at ORNL (Oak Ridge National Laboratory, USA). Measurements of the polycrystalline sample of $EuCu_2Si_2$ [74] were carried out at $T = 5$ K; the initial neutron energies were $E_i = 125$ meV and $E_i = 225$ meV, which provided an energy resolution with a full width at half maximum (FWHM) of 2 and 4 meV on the elastic line, respectively. The range of scattering angles was $2\theta = 4° - 58°$. The transmittance of the sample exceeded 90% even under the 'most adverse' conditions: $E_i = 125$ meV, final energy $E_f = 45$ meV, and scattering angle $2\theta = 57°$.

The energy spectra measured at $T = 5$ K for the minimum and maximum momentum transfers $Q_{min} = 0.6$ Å^{-1} and $Q_{max} = 10$ Å^{-1} after absorption correction are presented in Fig. 9a.

Note that the intensity of the peak M2 (37 meV) corresponds to the full intensity expected for the transition $J = 0 \to J = 1$ of the f^6 configuration, adjusted for the non-integer valence of europium. This implies that for f^6 the M1 peak at the lower energy cannot be directly related for this reason (in particular, as a result of the splitting in the CEF of the tetragonal symmetry for $J = 1$) to the spin-orbit excitation.

Figure 9b, where detailed measurements of the Q dependence of the magnetic scattering intensity are displayed, clearly shows that these peaks have different origins. One of them, located at a higher energy (M2, squares in Fig. 9b), corresponds to a spin-orbit intermultiplet transition, while the other peak at a lower energy (M1, dots in Fig. 9b) has a form factor corresponding to $\langle j_0(Q)\rangle$ and is most likely associated with the full wave function of the ground state — the 'resonant mode' — similar to the SmB_6 case. These considerations are discussed below.

Quasi-elastic scattering appears in the $EuCu_2Si_2$ spectrum at temperatures above 90 K, which is apparently associated with the closure of the spin gap, as in the case of SmB_6, and already at 150 K it reaches an intensity corresponding to the contribution expected from the Eu^{2+} configuration, taking into account the valence. The width of the quasielastic line is virtually independent of temperature (FWHM of about 22 meV). Unfortunately, due to experimental conditions, in particular, the unavailability of a single-crystal sample of $EuCu_2Si_2$, we could not reliably determine the nature of the Q dependence of the form factor of the quasielastic signal.

An increase in temperature starting from 80 K also leads to a decrease in the energy of both excitations, M1 and M2.

Moreover, the M1 energy decreases much faster than that of M2, while the width of both excitations increases sharply. As the analysis [72] showed, using the results of neutron studies of other Eu-systems 1−2−2 [69, 70], the change in the energy of M1 and M2 is interconnected and is most likely due to the Eu valence. In particular, extrapolation of the valence to $v = 3+$ yields an energy value for M2 of about 46 meV, which corresponds to the energy of the spin-orbit splitting of Eu^{3+}. It should be noted that for Sm the renormalization of the spin-orbit excitation was not observed at all in either Sm(La)B_6 or Sm(Y)S.

We now consider which model representations allow us to understand the above effects and their interrelation.

2.4 Model consideration: SmB_6 and Sm(Y)S

Among the most striking experimental effects discovered in the above-considered studies of the form factors of IV systems, we distinguish the detection of both a local maximum in the Q dependence of the quasielastic form factor in SmB_6 and 'resonant' modes with specific form factors in the spectra of IV compounds based on Sm and Eu, which are not associated with the spectra of each of the competing states separately. Note that the specific feature of the Q dependence of the quasielastic form factor for SmB_6 can logically be explained by a certain contribution from the f^5 configuration, the absence of which in other experimental data remained unclear for a long time.

The contribution of the Curie susceptibility of the f^5 component to the MFF for the quasielastic component of the neutron scattering spectrum in SmB_6 was explained on the basis of the exciton-polaron model presented in [54]. This microscopic model, based on the approach proposed in [75], makes it possible to represent the structure of the wave function for the Sm ion in the IV state. This representation provides an adequate description of the features of the excitation spectra of SmB_6 and Sm(Y)S observed experimentally, both for the dynamic magnetic susceptibility [54] and for the lattice dynamics [53].

In this model, the wave function of each samarium ion $\widetilde{\Psi}_m$ is a quantum-mechanically mixed state:

$$\widetilde{\Psi}_m = f^6_{J=0} f^*_{J=5/2} = v f^6_m + (1-v) f^5_m B^{(\mathrm{f})}_m , \tag{8}$$

where v is the relative content of Sm^{2+} ions in the compound, and $B^{(\mathrm{f})}_m$ describes the state of a weakly bound f-electron located near the rare-earth ion.

Thus, $\widetilde{\Psi}_m$ is a superposition of two states, f^6_m and $f^5_m B^{(\mathrm{f})}_m$, associated with two competing configurations, Sm^{2+} $|f^6_m, {}^7\mathrm{F}_0\rangle$ and Sm^{3+} $|f^5_m, {}^6\mathrm{H}_{5/2}\rangle$, which are not eigenstates of the full wave function (8). The manifestation of these configurations in the excitation spectrum in the form of broad (due to their short lifetime) peaks clearly follows from the experimental results [25, 29–31]. In [54], it was argued that it is the existence of a spatially extended component of $f^5_m B^{(\mathrm{f})}_m$ in the wave function that is responsible for the steeper decaying dependence on Q observed (Figs 7a and 8) for the exciton excitation realized in the spectrum as a 'resonant' mode with an energy of 14 meV in SmB_6 at a low temperature.

Closure of the spin gap when the system is heated to $T \geqslant 80$ K leads to a new regime in which the resonant mode is suppressed, and the quasielastic signal is restored. This indicates that the magnetic response is now determined by the 'parent' configurations (Sm^{2+} and Sm^{3+}). Consequently, it can be expected that the dependence of the quasielastic signal intensity on Q at a certain T takes the form

$$f^2_{\mathrm{QE}}(Q,T) = v \sum_i \sigma_{2,i}\, \rho_{2,i}(T,J) f^2_{2,i}(Q,T) + (1-v) \sum_i \sigma_{3,i}\, \rho_{3,i}(T,J) f^2_{3,i}(Q,T), \tag{9}$$

where v is the effective fraction of Sm^{2+} contained in Eqn (8), $\sigma_{2,i}$ ($\sigma_{3,i}$) are the cross sections of magnetic neutron scattering for various spin-orbit J multiplets of Sm^{2+} (Sm^{3+}), $f^2_{2,i}$ ($f^2_{3,i}$) are the corresponding MFFs calculated using Eqns (2) and (3), and $\rho_{2,i}$ ($\rho_{3,i}$) are the Boltzmann population factors. The last are calculated using the formula

$$\rho_k = \frac{g_k \exp(-E_k/k_{\mathrm{B}}T)}{\sum_k g_k \exp(-E_k/k_{\mathrm{B}}T)} , \tag{10}$$

where g_k is the multiplicity of the state with energy E_k, and T is the thermodynamic temperature.

Equation (9) allows the values of the MFF to be calculated using the original model (8) for the quasielastic signal in the IV state of Sm depending on the system temperature and its average valence. They are used further to analyze the features of the Q-dependence of the quasielastic signal intensity, i.e., the part of the dynamic susceptibility which is due to its Curie component.

As already noted, the MFF obtained from polarized neutron diffraction at $T = 7$ K (Fig. 8, squares) is associated with a fairly low magnetic moment $\mu \approx 0.02\mu_{\mathrm{B}}$. Given the experimental data, such a small value can be explained by only assuming that Sm has a singlet ground state separated by a gap of about 20 meV [56, 57] from the set of other f-electron states. In this situation, no contribution to the magnetic field-induced MFF at low temperatures should be expected from a specific state of the Sm^{3+} ion with $C_2 = 5.42$ (see (2), (3)).

The curves displayed in Fig. 8 show the results of calculations [12, 28, 76] of the static MFF $f^2(Q)$ $T \sim 0$ K for Sm^{2+} and Sm^{3+}. The induced MFF of SmB_6 ($T = 7$ K) measured in a magnetic field virtually coincides with the MFF for the intermultiplet transition [12] (Van Vleck component) with $C_2 = -1$ (see (2) and (3)). It should be mentioned that the results of measuring the Q-dependence for the intensities of intermultiplet transitions of the Sm^{2+} and Sm^{3+} configurations, obtained earlier in time-of-flight neutron experiments on a $^{154}Sm^{11}B_6$ polycrystal [30, 56], also turned out to be in good agreement with the calculated dependence for both configurations.

Another noteworthy point is the sharp decrease in the intensity of the extremely narrow (the width is determined by the spectrometer resolution) peak of the resonance mode, which exists up to about 50 K [56, 57]. This unusual behavior was interpreted in [57] as a sign of belonging to an excitation (exciton) associated with a partially delocalized state of the wave function corresponding to the ground IV state of the Sm ion (see above). This is probably a spin-orbit-type excitation, but specifically for the total wave function that includes the spatially extended component ($B^{(\mathrm{f})}_m$ in Eqn (8)) of the electron density [54]. Suppression of this excitation is apparently due to the closing of the gap in the spectrum of conduction electrons characteristic of the low-temperature state of SmB_6.

Such a representation of the nature of this excitation allows us to understand the reason for the evolution of the resonance mode in the experiment as the valence changes toward 2+. The monotonic change in both the form factor

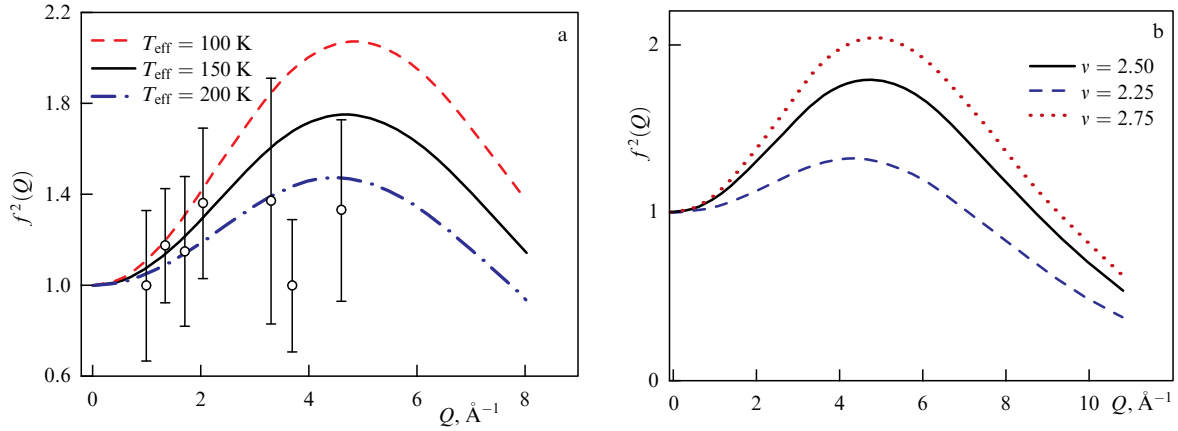

Figure 10. Comparison of experimental data ($T = 100$ K) for magnetic form factor of quasielastic scattering on SmB_6 (see Fig. 8) and results of MFF calculation (lines) using Eqn (9), where $T = 100$ K $+T_{\text{eff}}$: (a) for three effective temperatures T_{eff}: 100, 150, 200 K; (b) effect of changing average valence of Sm v on $f^2_{\text{QE}}(Q)$ calculated at fixed effective temperature $T_{\text{eff}} = 150$ K.

and the energy of the exciton peak (see Fig. 7) as the valence approaches 2+ is due to the corresponding transformation of the $B_m^{(\text{f})}$ component, namely, an increase in the degree of localization of the 'weakly bound' electron and the eventual formation from this component of the wave function (Eqn (8)) of a state identical to f^6.

It follows from the above that the closing of the gap in the electronic spectrum and the appearance of a quasielastic signal in the spectrum of electronic excitations of the IV-system SmB_6 at $T \geqslant 80$ K enable observation of the contribution from the form factor of the Sm^{3+} component (Curie type) in the neutron spectra. Indeed, the experimental dependence of the intensity of the quasielastic signal on Q differs qualitatively from all the others, as can be seen in Fig. 8 (circles corresponding to the spectra measured at $T = 100$ K). This experimental dependence can be compared with that predicted by Eqn (9). It should be noted that the use of the dipole approximation (Eqn (2)) for calculations rules out any inherent temperature dependence of these quantities (for example, due to CEF effects).

The issue of choosing the temperature parameter of the IV system to calculate the Boltzmann population coefficients in Eqn (9) is analyzed in detail in [59]. One of the common phenomenological approaches to the description of IV systems is to represent the effect of spin fluctuations (suppression of long-range magnetic order, finite magnetic susceptibility at $T \to 0$ in SmB_6 or Sm(Y)S, etc.) using an effective temperature T_{eff} due to the characteristic energy of quantum spin relaxation (spin fluctuations) E_{sf} in the 4f-electron system. T_{eff} can be determined experimentally from the line width of the corresponding component in the neutron spectra as $k_{\text{B}}T_{\text{eff}} = \Gamma/2$ (where Γ is the FWHM of the spectral line). In IV compounds, it can differ significantly from the actual (thermodynamic) temperature. For SmB_6, the characteristic energy of the spin fluctuation, estimated from the line width of either the quasielastic signal $\Gamma_{\text{QE}}/2k_{\text{B}} \approx 100$ K (see the inset in Fig. 8) or the spectral peaks of intermultiplet excitations $\Gamma_{\text{inter}}/2k_{\text{B}} \approx 200$ K at the experimental temperature $T = 10$ K [30, 56], significantly exceeds the thermal relaxation energy. This contrasts with 'normal' rare-earth systems, in which thermal spin fluctuations are usually one to two orders of magnitude lower than $k_{\text{B}}T$.

We now proceed to the experimental results in comparison with calculations based on Eqns (9) and (10) (symbols and lines, respectively, in Fig. 8) taking into account the parameter T_{eff} introduced above.

Figure 10a presents a comparison of the experiment and the calculation results, which, in accordance with T_{eff} and the thermal population factor, are primarily determined by the contributions from the states with $J = 1$ (Sm^{2+}) and $J = 5/2$, $7/2$ (Sm^{3+}), weighted with an average valence of $v \sim 2.5$, and neutron scattering cross sections ($\sigma_m(J = 1) = 2.7$ b, $\sigma_m(J = 5/2) = 0.4$ b, $\sigma_m(J = 7/2) = 6.2$ b). It is also shown how the form factor can look at the 'limiting' values of $T_{\text{eff}} = 100$–200 K. Taking into account the entire set of data, the value of $T_{\text{eff}} = 150$ K was chosen for the calculation of $f^2_{\text{QE}}(Q)$ as corresponding to real temperature conditions. As can be seen from Fig. 10a, the calculation in this temperature range is in reasonable agreement with the experiment and provides a justification of the noticeable discrepancy between the experimental quasielastic MFF and the results of measurements of other form factors. Thus, study [59] was the first to show that, under certain observation conditions for the IV ion Sm, the contribution from the Sm^{3+} configuration to the dependence of the MFF on the transferred neutron momentum Q is clearly present.

In addition to the temperature dependence, the dependence of the $f_{\text{QE}}(Q)$ shape on the average valence follows from representation (9). For SmB_6, this value is 2.5 ($v \sim 0.5$ in Eqn (9)); however, when Sm is replaced by La, it decreases, while when replaced by Ba or Ca, it increases. As shown in [29, 30], many characteristics of the magnetic excitation spectrum change, including the resonance mode MFF. Figure 10b displays the calculated effect of the average valence variation on the character of the Q dependence of the MFF for a quasielastic signal. It is qualitatively similar to the influence of the effective temperature variation. A comparison of the obtained dependence with the experiment is of interest for checking the adequacy of the approach we used to understand the physical nature of the MFF of a quasielastic signal. No experimental data for comparison are available as yet.

We now outline the concepts developed for Sm systems. The full wave function of the new state has its own excitation spectrum fundamentally containing two types of states [13], which are related either to charge redistribution (between the exciton and localized states) or only to a change in the mutual orientation of the spin and orbital moments. The latter type of

state determines the properties of the 'resonant' mode, essentially excitation from the true ground state of the IV ion ($J^* = 0$) to the first excited (exciton) state, which differs in the mutual orientation of the spin and orbital moments ($J^* = 1$). Since these are states of the full (true) wave function, the proper lifetime is consequently large (hence, particularly the small width of the resonant mode). In this case, the degree of electron delocalization $(1 - v)$ determines the degree of reduction in the spin-orbit excitation energy $J^* = 0 \rightarrow J^* = 1$ with respect to the excitation energy of 36 meV for a completely localized configuration corresponding to f^6.

A detailed discussion of many very interesting details of this approach is beyond the scope of this review. We only note in general terms that, based on the exciton model, it was possible to understand and quantitatively describe the anomalies of the electron–phonon interaction (for more details, see review [77]) and the main features of the spectrum of f-electron excitations of SmB_6 and Sm(Y)S [13], which has not been realized to date based on any other concepts. It turns out that new results for Eu-based systems can also be considered from the generalized positions of this concept (see Section 2.5).

2.5 Features of form factors in $EuCu_2Si_2$ spectra

As early as the initial stage of studies of the intermediate-valence compound $EuCu_2Si_2$, it was discovered that, when silicon is replaced by germanium in a certain region of silicon concentrations ($x \sim 0.75$), a ground state with features of a heavy-fermion state is realized [60]. A detailed study of the thermodynamic, magnetic, and kinetic properties of the full series of solid solutions $EuCu_2(Si_{1-x}Ge_x)_2$, carried out in [61], made it possible to propose a version of the phase diagram for the low-temperature region. The main result, confirmed by direct neutron diffraction measurements [73], is the presence of an extensive region with a magnetically ordered ground state, presumably the antiferromagnetic type, in a wide concentration range $(0 < x \leqslant 0.65)$ with a maximum $T_N \sim 14$ K, which was superimposed on the intermediate-valence state of Eu in the entire concentration range [61, 62]. In addition, the authors of [61] obtained unambiguous evidence of the formation of a heavy-fermion ground state for the concentration range $0.7 < x < 0.8$. A further increase in the silicon concentration, up to complete replacement of germanium, as shown by our results [71, 72], results in the formation of a low-temperature spin-gap state, which transforms into a state with strong spin fluctuations at temperatures above 100–150 K (for $EuCu_2Si_2$, the value $\Gamma_{QE}/2 \geqslant 120$ K was recorded). At all concentrations x, the system remained a metal.

The discovered coexistence of magnetically ordered and intermediate-valence states in a wide range of Ge concentrations is an extremely interesting and still unexplained phenomenon. The set of experimental results related to it, including neutron data, has been discussed recently [16]. It is clear that to solve this problem it is of importance, first and foremost, to have an adequate concept of the IV state of Eu. Its specific properties are most clearly exhibited in the region of high Si concentrations.

As already noted (end of Section 2.3.6), the IV state of europium is similar in some essential characteristics to the IV state of the samarium ion neighboring in the rare-earth series, but there are also significant differences [71, 72]. The neutron spectrum does not contain the peak of the inter-multiplet transition at an energy of 45 meV, which is characteristic of Eu^{3+} ($4f^6$), and the observed inelastic peaks undergo a very strong temperature evolution, altering their energy (shifting to the region of low energies) with an increase in temperature above 80 K, synchronously with the temperature change in the IV value.

An important feature of the magnetic excitation spectrum is the existence of two peaks in its inelastic part, which, judging by their characteristics (form factor (Fig. 9b), temperature dependence of position, intensity [72]), feature physically different origins. As shown in [72], their energy systematically depends on the valence of europium but is described by different power dependences, and the intensity of the peak at a higher energy (M2) fully corresponds to that expected for the spin-orbit excitation $^7F_0 \rightarrow {}^7F_1$ for Eu^{3+}, taking into account the average valence. These observations allowed us to assume that peak M2 corresponds to a 'renormalized' spin-orbit excitation associated with the $J = 0 \rightarrow J = 1$ transition in Eu^{3+}, while the M1 peak is a resonance mode due to the excitation spectrum from the true ground state of intermediate-valence europium with a mixed wave function, by analogy with SmB_6 or Sm(Y)S (see Section 2.4).

The experimental results show that, in the $EuCu_2Si_2$ case, the MFF characteristics of the 'resonant' mode (M1) turn out to be in some sense 'inverted' with respect to those discovered for SmB_6. We analyze below this set of experimental observations as regards the structure of the wave function of the IV state for the Eu ion.

The intensity of each peak as a function of the momentum transfer [74] is presented in Fig. 9b. An analysis of the MFF for the M2 peak at 37 meV (see the inset in Fig. 9a) shows that the experimental dependence of the intensity on the neutron momentum transfer corresponds to the calculated one for the spin-orbit excitation with $\Delta J = 1$ ($^7F_0 \rightarrow {}^7F_1$) for Eu^{3+} (see Eqn (2) for $C_2 = -1$). The experimental dependence on Q for the MFF of the M1 peak at 32 meV turns out to be nontrivial. Apparently, its intensity decreases more slowly than that of the form factor for M2 (Fig. 9b). Such behavior was not observed in the case of Sm-based IV systems, where electron delocalization naturally leads to a steeper decrease in the MFF with increasing Q. In this case, the Q dependence of the M1 form factor cannot be associated with any increase in the localization of f electrons and has a different origin. Indeed, the dependence on the wave vector can be very well described by the MFF for the f^7 configuration. The corresponding calculation is shown by the solid line in Fig. 9b for the MFF of the f^7-electron shell multiplet $f(Q) = j_0(Q)$ in the dipole representation (see Eqns (2) at $C_2 = 0$), which agrees very well with the experiment. Thus, the energies of the two peaks in the spectrum depend on the valence in a different way, and their intensities are related to MFFs of a different nature ($f_{M2}(Q) = \langle j_0(Q)\rangle - \langle j_2(Q)\rangle$ for M2 and $f_{M1}(Q) = \langle j_0(Q)\rangle$ for M1). This observation clearly indicates a difference between their physical natures.

Additionally, we note that the absolute values and the ratio of intensities rule out their direct connection with trivial effects of splitting in the crystal field.

In [72], it was suggested that, to describe the ground state of Eu with an intermediate valence, one can try to apply the 'hole' analogue of the wave function of type (8). In this case, the new quantum-mechanically mixed wave function of the ground state of the Eu ion can be represented as

$$\widetilde{\Psi}_m = v f_m^6 + (1 - v) f_m^7 B_m^{(h)} . \qquad (11)$$

As a result, for the wave function of the ground state of a system with an intermediate valence, we obtain a final formula consisting of two terms. The first of them is the usual state of the f^6 shell, while the second is partially delocalized, where $B_m^{(h)}$ corresponds to the state of the hole exciton associated with the f^7 state and is responsible for the partially frozen orbital moment of the entire composite wave function, which is completely absent for the pure f^7 state.

The excitation spectrum of the wave function of the ground state (11) is determined by the state of the weakly bound exciton, which sets the energy and form factor of the resonance mode and the 'parent' excitations with their form factors. The latter, by analogy with the case of Sm-based systems, correspond to the excitation spectra of the f^n and f^{n+1} configurations. The f^7 state, as noted above, does not 'generate' an inelastic component in the spectra; therefore, the spectrum (at $T = 5$ K) is represented by only two peaks. The highest energy peak M2 with an energy of 37 meV corresponds to the initial f^6 state, but its energy (unlike the case of Sm) depends on the valence (see below), and its form factor (2) (as it should be for a spin-orbit excitation with $C_2 = -1$ [20]) is determined by the formula $f(Q) = \langle j_0(Q)\rangle - \langle j_2(Q)\rangle$ (see Fig. 9). A similar type of Q-dependence for the peaks at 36 meV (f^6 configuration) and 125 meV (f^5 configuration) was observed for samarium compounds [56].

The other peak (M1), at 32 meV, is a resonance-type excitation. An important feature of this new excitation, associated with the internal structure of the corresponding state of the total wave function, is its magnetic form factor.

In the case of the samarium ion, the form factor for resonant excitation decreases sharply with increasing modulus of the wave vector Q. Physically, this is due to the spatially distributed density of states of the sixth f-electron, which is weakly bound to the f^5 shell of the Sm ion. In the corresponding expression for the wave function (2), this weakly bound state was represented by the term $\langle f^5 B_m\rangle$, corresponding to the exciton state.

In the case of europium, similarly to Sm systems, we are dealing with a weakly bound state of the 'hole' and the f^7 state (Eqn (11)) in the form $\langle f^7 B_m\rangle$. However, the neutron cannot interact with the hole; therefore, the form factor for the corresponding excitation from the ground state of the full wave function (11) is determined in this case by the properties of the ion core. Consequently, the orbital momentum for $\langle f^7 B_m\rangle$ is effectively suppressed ($L = 0$), as is realized for the 'pure' f^7 state. Thus, the form factor loses its orbital component and turns out to be linked to only $\langle j_0\rangle$, as it should be for the f^7 configuration. Naturally, in the experiment, this led to a weaker dependence of the peak intensity on Q than for the 'usual' spin-orbit excitation $J = 0 \to J = 1$ for the f-shell with $L \neq 0$. This mechanism explains the apparent difference between the Q dependences of the intensity for the two inelastic peaks in the spectrum of $EuCu_2Si_2$, which was observed experimentally (see Fig. 9).

Here, we only discussed the Q dependences of the intensities in the Eu 1−2−2 spectra, without addressing some other interesting and significant experimental results noted above. A detailed discussion of the conditions for the formation of the IV state for europium and possible mechanisms of the renormalization of the energies of the M1 and M2 peaks with a change in valence is presented in [74].

3. Conclusions

The analysis of the results of neutron measurements of the magnetic form factor for rare-earth systems with intermediate valence reviewed here shows that an important role in such studies is played by taking into account the microscopic nature of the magnetic moment of the electron shell interacting with the neutron, the ratio between its Curie and Van Vleck components. Of great importance in the analysis of the results of the diffraction method for measuring the MFF is the nature of the ground state itself and the physical nature of the excitation spectrum, which is especially clearly exhibited in spectroscopic measurements. Thus, by analyzing the results of these experiments, it is possible to obtain unique information about the nature and structure of the wave function of the f-electron shell responsible for the formation of the IV state.

Among the experiments performed to date on the study of the MFF of RE intermetallics, the most significant results have been obtained for systems based on RE elements of the middle of the series. Detailed studies of the MFF using elastic and inelastic neutron scattering of systems based on RE ions of Sm and Eu enabled the establishment of both the common nature of the IV state for them and the fundamentally important differences that determine the specific features of their physical properties. As regards model concepts, experimental information on the qualitative differences in the MFF specific to various components of the f-electron excitation spectrum confirmed the realism of the exciton-polaron model as applied to samarium-based systems and made it possible to extend it to some europium intermetallics.

A number of the discovered physical phenomena, for example, significant renormalization of the spin-orbit excitation energy of Eu with a change in its valence, and the behavioral features of the resonance mode in Sm and Eu systems, require further exploration and analysis. For now, we can only assume that this is due to the different roles of Coulomb and hybridization interactions [74] for these two types of systems in the formation of the IV state.

It is of importance that the approach implemented in the reviewed studies provides a deeper physical understanding of the IV phenomenon, which was initially presented as a direct result of some fairly fast fluctuations between the states of the RE ion, simply differing by one in the number of f-electrons. It is also significant that this approach is formulated on the basis of detailed neutron spectroscopic studies, whose use provides information on f-electron states at the microscopic level, significantly complementing the data of X-ray and gamma resonance spectroscopy.

Acknowledgments. The authors are grateful to A.P. Menushenkov for his interest and support of the work and E.S. Klementyev for fruitful discussions.

The work was supported by the Ministry of Science and Higher Education of the Russian Federation (Agreement No. 075-15-2021-1352).

References

1. Coleman P *Philos. Mag.* **97** 3527 (2017)
2. v. Löhneysen H *Physica B* **378–380** 1170 (2006)
3. Loewenhaupt M, Fischer K H, in *Handbook on the Physics and Chemistry of Rare Earths* Vol. 16 (Eds K A Gschneidner (Jr.), L Eyring) (Amsterdam: Elsevier, 1993) p. 1, https://doi.org/10.1016/S0168-1273(05)80016-9

4. Lander G H, in *Handbook on the Physics and Chemistry of Rare Earths* Vol. 17 (Eds K A Gschneidner (Jr.), L Eyring, G H Lander, G R Choppin) (Amsterdam: Elsevier, 1993) p. 635, https://doi.org/10.1016/S0168-1273(05)80034-0
5. Hirst L L *Adv. Phys.* **27** 231 (1978)
6. Mirmelstein A V, Clementyev E S, Kerbel O V *JETP Lett.* **90** 485 (2009); *Pis'ma Zh. Eksp. Teor. Fiz.* **90** 531 (2009)
7. Elliott R J (Ed.) *Magnetic Properties of Rare Earth Metals* (New York: Springer, 2013) https://doi.org/10.1007/978-1-4757-5691-3
8. Freeman A J, Watson R E *Phys. Rev.* **127** 2058 (1962)
9. Gurevich I I, Tarasov L V *Low-Energy Neutron Physics* (Amsterdam: North-Holland Publ. Co., 1968); Translated from Russian: *Fizika Neitronov Nizkikh Energii* (Moscow: Nauka, 1965)
10. Squires G L *Introduction to the Theory of Thermal Neutron Scattering* (Mineola, NY: Dover Publ., 1996)
11. Ivanov A S, Alekseev P A *Crystallogr. Rep.* **67** 18 (2022); *Kristallografiya* **67** 21 (2022)
12. Osborn R et al., in *Handbook on the Physics and Chemistry of Rare Earths* Vol. 14 (Eds K A Gschneidner (Jr.), L Eyring) (Amsterdam: Elsevier, 1991) p. 1, https://doi.org/10.1016/S0168-1273(05)80099-6
13. Alekseev P A *Phys. Usp.* **60** 58 (2017); *Usp. Fiz. Nauk* **187** 65 (2017)
14. Marshall W, Lovesey S W *Theory of Thermal Neutron Scattering: the Use of Neutrons for the Investigation of Condensed Matter* (Oxford: Clarendon Press, 1971)
15. Wachter P, in *Handbook on the Physics and Chemistry of Rare Earths* Vol. 19 (Eds K A Gschneidner (Jr.) et al.) (Amsterdam: Elsevier, 1994) p. 177
16. Savchenkov P S, Alekseev P A *Crystals* **13** 1238 (2023)
17. Taylor K N R, Darby M I *Physics of Rare Earth Solids* (London: Chapman and Hall, 1972); Translated into Russian: *Fizika Redkozemel'nykh Soedinenii* (Moscow: Mir, 1974)
18. Boucherle J X, Givord D, Schweizer J *J. Phys. Colloq.* **43** C7-199 (1982)
19. Blume M, Freeman A J, Watson R E *J. Chem. Phys.* **37** 1245 (1962)
20. Balcar E, Lovesey S W, Wedgwood F A *J. Phys. C* **3** 1292 (1970)
21. Boucherle J X, Schweizer J *Physica B + C* **130** 337 (1985)
22. Balcar E, Lovesey S W *J. Phys. C* **19** 4605 (1986)
23. Boucherle J-X et al. *Physica B* **206–207** 374 (1995)
24. Holland-Moritz E, Wohlleben D, Loewenhaupt M *Phys. Rev. B* **25** 7482 (1982)
25. Alekseev P A et al. *Europhys. Lett.* **23** 347 (1993)
26. Murani A P "Neutron spectroscopy of valence fluctuation compounds of cerium and ytterbium," in *Concepts in Electron Correlation* (NATO Science Ser., Vol. 110, Eds A C Hewson, V Zlatić) (Dordrecht: Springer, 2003) p. 297, https://doi.org/10.1007/978-94-010-0213-4_29
27. Murani A P et al. *Phys. Rev. B* **48** 10606 (1993)
28. Moon R M et al. *J. Appl. Phys.* **49** 2107 (1978)
29. Alekseev P A et al. *J. Exp. Theor. Phys.* **81** 586 (1995); *Zh. Eksp. Teor. Fiz.* **108** 1064 (1995)
30. Alekseev P A et al. *Physica B* **259–261** 351 (1999)
31. Alekseev P A et al. *Phys. Rev. B* **74** 035114 (2006)
32. Shapiro S M, Birgeneau R J, Bucher E *Phys. Rev. Lett.* **34** 470 (1975)
33. Møller H B, Shapiro S M, Birgeneau R J *Phys. Rev. Lett.* **39** 1021 (1977)
34. Vainshtein É E, Blokhin S M, Paderno Yu B *Sov. Phys. Solid State* **6** 2318 (1965); *Fiz. Tverd. Tela* **6** 2909 (1964)
35. Alekseev P A, Lazukov V N, Sadikov I P, in *Rare-Earth Borides* (Ed. D Inosov) (New York: Jenny Stanford Publ., 2021) p. 489
36. Stassis C et al. *J. Appl. Phys.* **53** 7890 (1982)
37. Stassis C et al. *J. Appl. Phys.* **50** 2091 (1979)
38. Moon R M, Koehler W C *J. Appl. Phys.* **50** 2089 (1979)
39. Severing A et al. *Phys. Rev. B* **41** 1739 (1990)
40. Zwicknagl G, Zevin V, Fulde P *Z. Phys. B* **83** 153 (1991)
41. Currat R et al. *Physica B* **156–157** 812 (1989)
42. Holland-Moritz E, in *Valence Instabilities: Proc. of the Intern. Conf., Zürich, Switzerland, April 13–16, 1982* (Eds P Wachter, H Boppart) (Amsterdam: North-Holland, 1982) p. 347
43. Alekseev P A, Lazukov V N, Savchenkov P S *J. Surf. Investig. X-Ray Synchrotron Neutron Tech.* **16** 303 (2022)
44. Christianson A D et al. *Phys. Rev. Lett.* **96** 117206 (2006)
45. Bouvet A et al. *J. Phys. Condens. Matter* **10** 5667 (1998)
46. Nefeodova E V et al. *Phys. Rev. B* **60** 13507 (1999)
47. Liu S H *Phys. Rev. B* **63** 115108 (2001)
48. Nemkovski K S et al. *Phys. Rev. Lett.* **99** 137204 (2007)
49. Alekseev P A et al. *J. Exp. Theor. Phys.* **124** 957 (2017); *Zh. Eksp. Teor. Fiz.* **151** 1120 (2017)
50. Nemkovski K S et al. *Phys. Solid State* **52** 936 (2010); *Fiz. Tverd. Tela* **52** 878 (2010)
51. Alekseev P A et al. *Phys. Rev. B* **89** 115121 (2014)
52. Moon R M, Liu S H, Werner K *J. Magn. Magn. Mater.* **31–34** 387 (1983)
53. Kikoin K A, Mishchenko A S *J. Exp. Theor. Phys.* **77** 828 (1993); *Zh. Eksp. Teor. Fiz.* **104** 3810 (1993)
54. Kikoin K A, Mishchenko A S *J. Phys. Condens. Matter* **7** 307 (1995)
55. Emi N et al. *Phys. Rev. B* **97** 161116 (2018)
56. Alekseev P A et al. *J. Phys. Condens. Matter* **7** 289 (1995)
57. Alekseev P A et al. *J. Solid State Chem.* **133** 230 (1997)
58. Fuhrman W T et al. *Phys. Rev. Lett.* **114** 036401 (2015)
59. Alekseev P A et al. *JETP Lett.* **103** 636 (2016); *Pis'ma Zh. Eksp. Teor. Fiz.* **103** 720 (2016)
60. Levin E M et al. *Phys. Status Solidi B* **161** 783 (1990)
61. Hossain Z et al. *Phys. Rev. B* **69** 014422 (2004)
62. Fukuda S et al. *Acta Phys. Polon. B* **34** 1177 (2003)
63. Ahmida M A et al. *Phys. Rev. B* **102** 155110 (2020)
64. Ahmida M A et al. *Phys. Rev. B* **101** 205127 (2020)
65. Wolf B et al. *Phys. Rev. B* **107** 245147 (2023)
66. Kuzhel B et al. *Adv. Condens. Matter Phys.* **2024** 5127659 (2024)
67. Song Y-J et al. *Phys. Rev. B* **107** 075149 (2023)
68. Swami R, Hooda M K, Hossain Z *J. Magn. Magn. Mater.* **589** 171517 (2024)
69. Holland-Moritz E et al. *Phys. Rev. B* **35** 3122 (1987)
70. Holland-Moritz E et al. *Z. Phys. B* **77** 105 (1989)
71. Alekseev P A et al. *J. Exp. Theor. Phys.* **105** 14 (2007); *Zh. Eksp. Teor. Fiz.* **132** 22 (2007)
72. Alekseev P A et al. *J. Phys. Condens. Matter* **24** 375601 (2012)
73. Nemkovski K S et al. *Phys. Rev. B* **94** 195101 (2016)
74. Savchenkov P S et al. *J. Phys. Condens. Matter* **30** 055801 (2018)
75. Stevens K W H *J. Phys. C* **9** 1417 (1976)
76. de Wijn H W, van Diepen A M, Buschow K H J *Solid State Commun.* **15** 583 (1974)
77. Alekseev P A *Phys. Usp.* **58** 330 (2015); *Usp. Fiz. Nauk* **185** 353 (2015)